SIMEC, An Environment Correction For MERIS Based On The NIR Similarity Spectrum

Els Knaeps, Sindy Sterckx, Flemish Institute for Technological Research (VITO), Remote Sensing Unit (TAP), Boeretang 200, B-2400 Mol, Belgium.

Kevin Ruddick, Management Unit of the North Sea Mathematical Models (MUMM), Royal Belgian Institute for Natural Sciences (RBINS), 100 Gulledelle, B-1200 Brussels, Belgium.

Claudia Giardino, Bresciani Mariano, Optical Remote Sensing Group, CNR-IREA, Via Bassini 15, 20133 Milano, Italy

INTRODUCTION

In many coastal and inland waters environment effects hamper the correct retrieval of water quality and aerosol parameters from remotely sensed imagery. Environment effects can be observed as a blurring effect caused by scattering in the atmosphere of the highly contrasting dark waters and bright land, particularly if vegetated. As the contrast is highest in the Near Infrared (NIR) the blurring effect is most visible in these NIR wavelengths. Several modeling studies have shown the dependence of the adjacency effect on mainly the aerosol optical thickness (AOT) and aerosol vertical distribution (Santer and Schmechtig 2000, Minomura *et al.* 2001).
Corrections have been proposed for these environment effects using simulations and a LUT approach. For MERIS imagery Santer *et al*. (2009) proposed a method based on the single scattering approximation. This correction procedure, named ICOL (Improving Contrast between Ocean and Land) is integrated into the BEAM toolbox for the correction of MERIS imagery. According to Ruiz-Verdú *et al*. (2008) ICOL pre-processing has a neutral or positive effect in the estimation of water leaving reflectance, depending on the lake type.

Recently a new environment correction has been proposed for hyperspectral airborne datasets based on the correspondence with the NIR similarity spectrum (Sterckx *et al.*, 2010). The NIR similarity spectrum provided a basis to both detect and correct adjacency effects. Detection of the magnitude of the environment effects is based on the deviations from the NIR similarity spectrum. The detection was tested on airborne hyperspectral datasets from two different sites and flown at different flight altitude. The adjacency correction algorithm estimates the contribution of the background radiance based on the correspondence with the NIR similarity spectrum. Again the correction was tested on the same test imagery and validated using in-situ water-leaving reflectance measurements. A key aspect of the method is that no assumptions have to be made on the NIR albedo, such that the correction can be applied over more turbid waters, i.e up to the limit of validity of the similarity spectrum (0.3 to 200 mg/l according to Ruddick *et al.*, 2006).
In this paper the NIR similarity correction is adjusted for MERIS imagery and is referred to as SIMEC (SIMilarity Environment Correction). Details are provided on the adjusted method. The

method is tested on a dataset of lake Trasimeno. The results are compared with the ICOL adjacency correction, which is implemented in BEAM.

NIR SIMILARITY SPECTRUM

The method is based on the invariant shape of the water-leaving reflectance of the NIR (700-900 nm). This invariant shape was defined by Ruddick *et al.* (2006) by normalization at 780nm and referred to as NIR similarity spectrum:

$$\overline{R_{wn}}_{780}(\lambda) = \frac{R_W(\lambda)}{R_W(780)} \tag{1}$$

With $R_w(\lambda)$ the water-leaving reflectance. This similarity spectrum is valid for almost any water body with turbidity ranging from moderately turbid (SPM concentration 0.3 g m^{-3}) to extremely turbid (200 g m^{-3}) and is tabulated by Ruddick *et al.* (2006).

MODTRAN ATMOSPHERIC CORRECTION PROCEDURE FOR MERIS

The atmospheric correction procedure is based on Modtran4 and the interrogation technique of De haan and Kokke (1996). The complete atmospheric correction procedure is detailed in Sterckx *et al.* (2010) and can be brought back to the following expression:

$$R_{app} = \frac{c_1 + c_2 L^{rs}_{target} + c_3 L^{rs}_{backgr}}{c_4 + c_5 L^{rs}_{backgr}} \tag{2}$$

with

$c_1 = -L_{atm-path}$

$c_2 = 1 + t_{dif}(\tau,\theta_V)/t_{dir}(\tau,\theta_V)$

$c_3 = -t_{dif}(\tau,\theta_V)/t_{dir}(\tau,\theta_V) = 1 - c_2$

$c_4 = t(\theta_S)F_0\cos(\theta_S)t(\tau,\theta_V)/\pi - s^* L_{atm-path}$

$c_5 = s^*$

R_{app} is the target apparent reflectance, L^{rs}_{target} is the radiance received by the sensor and L^{rs}_{backgr} is the average radiance detected by the sensor for the background. $L_{atm-path}$ is the atmospheric path radiance, t_{dif} and t_{dir} are respectively the diffuse and direct ground-to-sensor transmittance, θ_S and φ_S are respectively the sun zenith and azimuth angle, θv and φ_V are respectively the viewing zenith and azimuth angle, $s*$ the spherical albedo of the atmosphere. The water leaving reflectance R_W can be retrieved from R_{app} as follows:

$$R_W = R_{app} - d_1 \tag{3}$$

with $d_1 = \pi r(\theta_v) L_{sky}(a) / E_d(a)$ (4)

$L_{sky}(a)$ is the downwelling sky radiance, $E_d(a)$ is the downwelling irradiance above the surface and r is the Fresnel reflection coefficient. The $c_{1..5}$ parameters can be derived by running MODTRAN4 for three different surface albedo's: 0, 0.5 and 1. An estimation of the d_1 parameter requires two MODTRAN4 runs with the sensor respectively looking to the sky for $L_{sky}(a)$ and to the surface for $E_d(a)$.

Instead of a pixel wise 'water-based' aerosol retrieval this method proposes a land based estimate or, when available, derivation of aerosol from sunphotometer readings. The method currently incorporated in the Central Data Processing Centre (CDPC) of VITO is based on the selection of Dense Dark Vegetation (DDV) targets and some assumptions on their Red and NIR albedo (Richter *et al*., 2006). An alternative method is presented by Guanter *et al*. (2010). As these 'land methods' provide an average value of the visibility or Aerosol Optical Thickness (AOT) for the entire scene, they can fail in the case of inhomogeneous atmospheric conditions. However, using these methods we do not have to make any assumptions on the NIR albedo of the water and these wavelengths can therefore be used for quality control or adjacency corrections. Additionally, according to Guanter *et al*. (2010), the accuracy of this method for very complex water bodies may outperform that of approaches based on the inversion of site-specific bio-optical models which are not prepared to cover a wide range of water conditions

For MERIS imagery in particular the Thuillier irradiance file was used instead of the Standard Modtran irradiance file for airborne datasets and the complete sensor and sun geometry is included in the correction procedure.

DETECTION OF ADJACENCY EFFECTS IN MERIS IMAGES

Environment effects are most pronounced when water pixels are surrounded by vegetated land. In the NIR the vegetation spectrum shows a sharp increase in reflectance (the red-edge). This high reflectance in the NIR is in sharp contrast with the low water reflectances in the NIR (Figure 1). When the vegetation spectrum contributes reflectance to the water spectrum through scattering in the atmosphere it not only increases the reflectance in the NIR but it also alters the shape to something different from the NIR similarity spectrum . A larger deviation from the NIR similarity spectrum is an indication of increased adjacency effects.

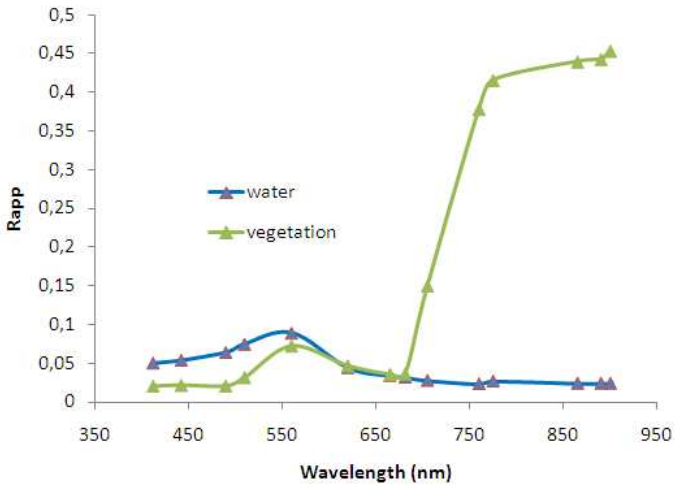

Figure1: Water and vegetation spectra in a MERIS image

To detect these adjacency effects in MERIS imagery an atmospheric correction based on the Modtran interrogation technique is performed on the imagery neglecting adjacency effects. After atmospheric correction the spectra are normalized at 775 nm. From these normalized spectra one or several suitable wavelengths need to be selected that can be compared to the NIR similarity spectrum. Sterckx *et al*. (2010) defined some basic rules for this wavelength selection: (1) the selected wavelengths cannot be influenced by water vapor or oxygen absorption, (2) they should not be located before 690 nm because of the large standard deviation of the NIR similarity spectrum and (3) they are preferably located in the red-edge region of the spectrum. Considering these rules, the 709 nm band was found to be most suitable for MERIS imagery. Having found a suitable wavelength, the error due to adjacency effects can then be calculated as follows (Ruddick *et al.*, 2005):

$$\varepsilon(\lambda_i,775)=\frac{\overline{R_{wn\ 780}}(709)R_w^{retrieved}(775)-R_w^{retrieved}(709)}{\overline{R_{wn\ 780}}(709)-1} \tag{5}$$

with $R_{wn\ 780}(\lambda_i)$ taken from the tabulated NIR similarity spectrum (Ruddick *et al.*, 2006) and $R_{w\_retrieved}$ the retrieved measured water leaving reflectance.

SIMEC CORRECTION

To correct for adjacency effects, the average radiance detected by the sensor for the background, defined in (2), has to be calculated. This background radiance is a weighted average of the pixel radiance values surrounding the target pixel:

$$L_{\text{backgr}}^{rs}=\sum_{i=0}^{i=X} w_{i*}\overline{L_i} \tag{6}$$

where $\overline{L_i}$ is the mean radiance of the additional background pixels at range i. $\overline{L_0}$ is the radiance of the target pixel. X is the range of the adjacency effect expressed in pixels.

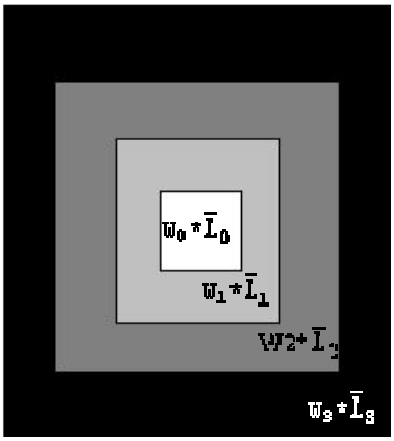

Figure 2: Example of background calculation for a pixel with a background range X = 3 pixels

The maximum range has been set to 30km which equals a 100 pixel range for a spatial resolution of 300m. With increasing distance from the target pixel the weights decrease. The weights for each pixel are calculated as follows:

$$wi = \frac{\omega_i}{\sum_{i=1}^{100} \omega_i}$$

$$\omega_i = \int_{x_{i-1}}^{x_i} A_x * \left(1 - \frac{t_d^a * F^a(x) + t_d^r * F^r(x)}{t_d^a + t_d^r}\right) dx \qquad (7)$$

$F^a(x)$ = 1 - (0.448 * exp (-0.27 * x*S) + 0.552 * exp (- 2.83 * x*S))

$F^r(x)$= 1 - (0.930 * exp (-0.08 * x*S) + 0.07 * exp (- 1.1 * x*S))

t_d^a= 0.200202

t_d^r = 0.011312

A_x= (2*S*x +S)*(2*S*x +S) - (2*S*(x-1)+S)*(2*S*(x-1)+S)

$F^r(x)$ and $F^a(x)$ correspond to the environment function for Rayleigh and aerosol scattering as specified in 6S (Vermote *et al.*, 1994). t_d^r and t_d^a are the diffuse transmissions (from target to sensor) for respectively Rayleigh and aerosols and are calculated using Modtran. S is the spatial resolution expressed in km.

The unknown in these expressions is X, the range of the adjacency effect expressed in pixels. This range can be estimated iteratively using the NIR similarity spectrum.
For each pixel the procedure starts with a range equal to 0, which corresponds with no adjacency effect. The range is then subsequently expended until the following formulation is true:

$$Nirsim - 1Stdev \le \frac{\left[\frac{c_1 + c_2 L^{rs}_{target} + c_3\left(L^{rs}_{backgr}\right)}{c_4 + c_5\left(L^{rs}_{backgr}\right)} - d_1\right]_{709\,nm}}{\left[\frac{c_1 + c_2 L^{rs}_{target} + c_3\left(L^{rs}_{backgr}\right)}{c_4 + c_5\left(L^{rs}_{backgr}\right)} - d_1\right]_{775nm}} \le Nirsim + 1Stdev \quad (8)$$

In addition the range will stop expanding in one direction when it reaches the borders of the imagery.

TEST DATASET

The methodology is tested for lake Trasimeno in central Italy (Figure 3). Lake Trasimeno is a shallow (average depth of 4 m) and meso-eutrophic lake, characterized by turbid waters (average Secchi disk depth 1 m). A MERIS image from the lake was acquired on May 17, 2009. Some water reflectance data are available from May 12, 2009. They were derived by underwater downwelling irradiance and upwelling radiance ASD-FR measurements, subsequently corrected for the immersion factor. Visibility is derived from sunphotometer readings.

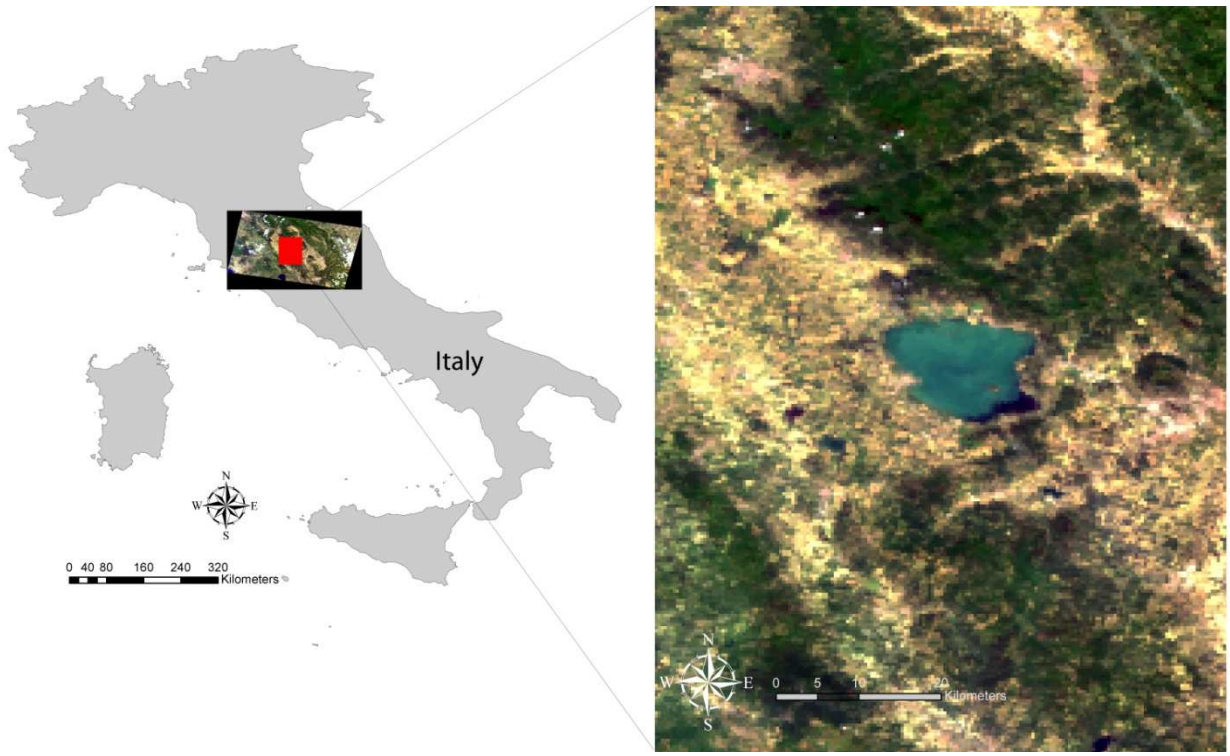

Figure 3: lake Trasimeno

Figure 4 shows the results of the adjacency detection using the NIR similarity spectrum. The highest errors are observed close to the border of the lake and the errors decrease gradually towards the centre. The southeast part of the lake (darker area in Figure 4a) is further excluded from the analysis as the reflectance spectra give evidence of some irregularities that could be due to bottom effects.

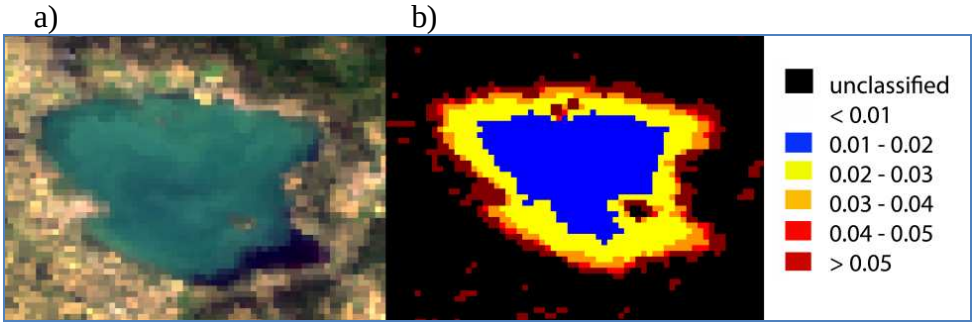

Figure 4: Adjacency detection for lake Trasimeno [Figure 4a is a true color composite of the lake and Figure 4b is the error map]

VALIDATION AND INTERCOMPARISON

The atmospheric and adjacency correction based on Modtran are compared with correction procedures available in the BEAM toolbox. Using this toolbox atmospherically corrected surface reflectance is obtained by running the BEAM Regional Case 2 Water (C2R) processor (version 1.4) which applies an atmospheric correction based on a neural network approach (Doerffer and Schiller, 2008). The neural network takes the influence of aerosols, thin cirrus clouds, sun and sky glint and the water leaving radiance into account. The forward model is a Monte Carlo photon tracing model, which describes the radiative transfer within the ocean-atmosphere system. The water part was not used and the water leaving radiance was computed with a forward NN, trained with spectra computed with Hydrolight. Adjacency correction in BEAM is performed using ICOL (Improved Contrast between Ocean and Land, version 1.0.4, Santer *et al.*, 2007). ICOL performs adjacency effect corrections for a two layer model using a look-up-table simulated with the primary scattering approximation (Santer & Schmechtig, 2000). The regular Rayleigh correction is applied for all pixels (land, clouds and water), while the rest of the procedure is only applied to water pixels within 30 km from the shore. The aerosol vertical scale height is set to 3km, the aerosol type and optical thickness (AOT) are derived from the image using bands 12 and 13. All bands are converted back into at-sensor radiances (L1C).

A workflow is followed as detailed in Figure 5. First the TOA L1B data are processed with C2R and Modtran without ICOL correction. This results in remote sensing reflectance Rrs (processed with C2R) or water-leaving reflectance Rw (processed with Modtran). Then the same procedure is followed but using ICOL as a preprocessing step. Finally the SIMEC correction was applied to the TOA L1B data resulting in a water-leaving reflectance data corrected for adjacency effects. To be consistent with the ICOL correction this dataset is converted back to TOA radiance neglecting adjacency effects. Again the C2R and Modtran atmospheric corrections are applied to retrieve remote sensing or water-leaving reflectance data.

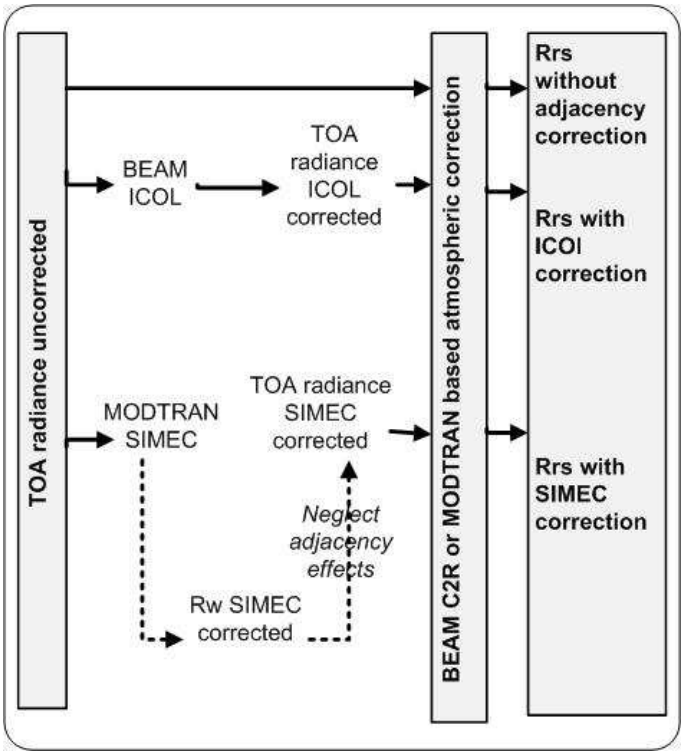

Figure 5: Validation workflow

RESULTS

Using the workflow detailed in Figure 5 two comparison exercises can be made: a comparison at TOA radiance level (Figure 6) and a comparison at Rw/Rrs level (Figure 7).

For the comparison at TOA level, average background spectra are extracted from the image. These spectra are not the ones used in the correction procedure but they are presented here to better interpret the effect of the surroundings and to judge on the quality of the adjacency corrections. They are presented in Figure 6 for a box of 20 by 20, 50 by 50 and 100 by 100 pixels. The shape of these spectra clearly indicates the presence of vegetation in the surroundings of the lake. The higher radiance values for the 100 by 100 average are due to the higher percentage of land and the smaller percentage of water within the bounding box. Both the uncorrected spectra and the corrected spectra using SIMEC and ICOL are shown. The results obtained with the SIMEC correction agree quite well with the ICOL corrected spectrum. Both adjacency corrections lower the spectrum in the NIR although the effect of SIMEC is stronger. Between 412 and 560 nm the ICOL corrected spectrum is higher than SIMEC and the uncorrected spectrum. Deviations between ICOL and SIMEC can partly be attributed to the Fresnel land mask (reduction of surface reflection over adjacency land), which is only taken into account by ICOL.

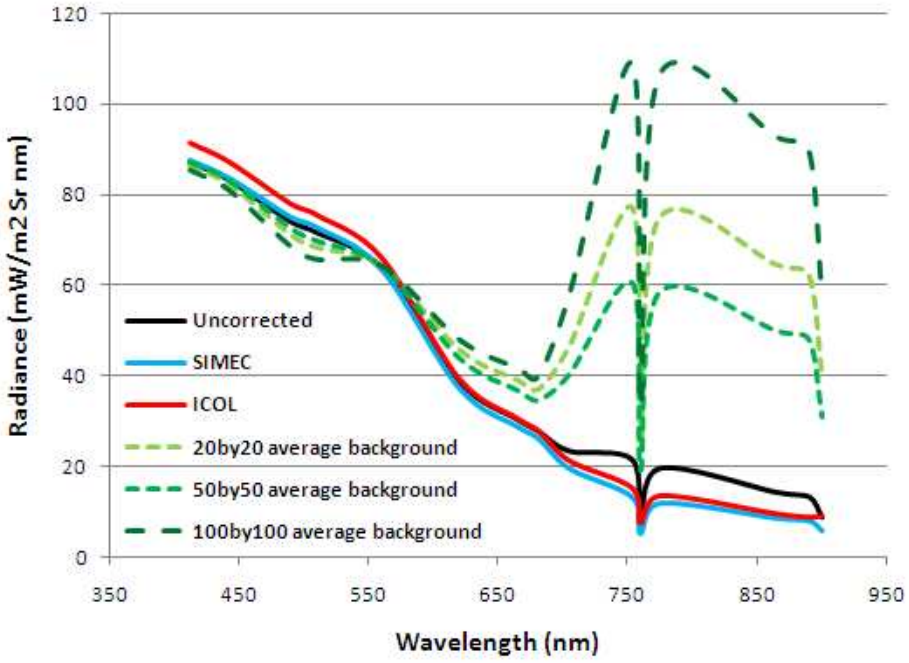

Figure 6: Comparison at TOA level

For the comparison at Rw/ Rrs level, the water-leaving and remote sensing reflectance spectra are additionally compared with in-situ spectra. The water-leaving reflectance spectra at the left are processed with Modtran. Here, the shape of the vegetation is recognizable in the uncorrected spectra. In the remote sensing reflectance spectra, processed with C2R, this particular shape is not visible. Even for spectra with pronounced adjacency effects C2R will result in a spectrum that 'looks' like water since it is trained with water spectra. However this water spectrum might not reflect the real optical properties and constituents of the water or it may result in erroneous estimates of the atmospheric parameters. For BEAM-C2R SIMEC and ICOL are very much the same over the entire wavelength range. For Modtran differences are more apparent. In general there is a decrease in the water-leaving reflectance in the NIR after both correction procedures giving a better closure with the in-situ spectra. For SIMEC no significant variation from the uncorrected spectrum can be observed in the blue. Looking at the BEAM-C2R results the adjacency corrections increase the reflectance between 400 and 750 nm and for case b) and c) better match the in- situ spectra. For case a) the optical closure between in-situ and image spectra improves in the red and NIR but there is still a large offset in the blue. In case b) the corrected MERIS spectra are still largely overestimated with respect to the in-situ data. Differences between in-situ and image spectra can partly be attributed to match up problems (spatial variation within one pixel, timing of both measurements,..).

CDPC – Modtran BEAM – C2R

a)

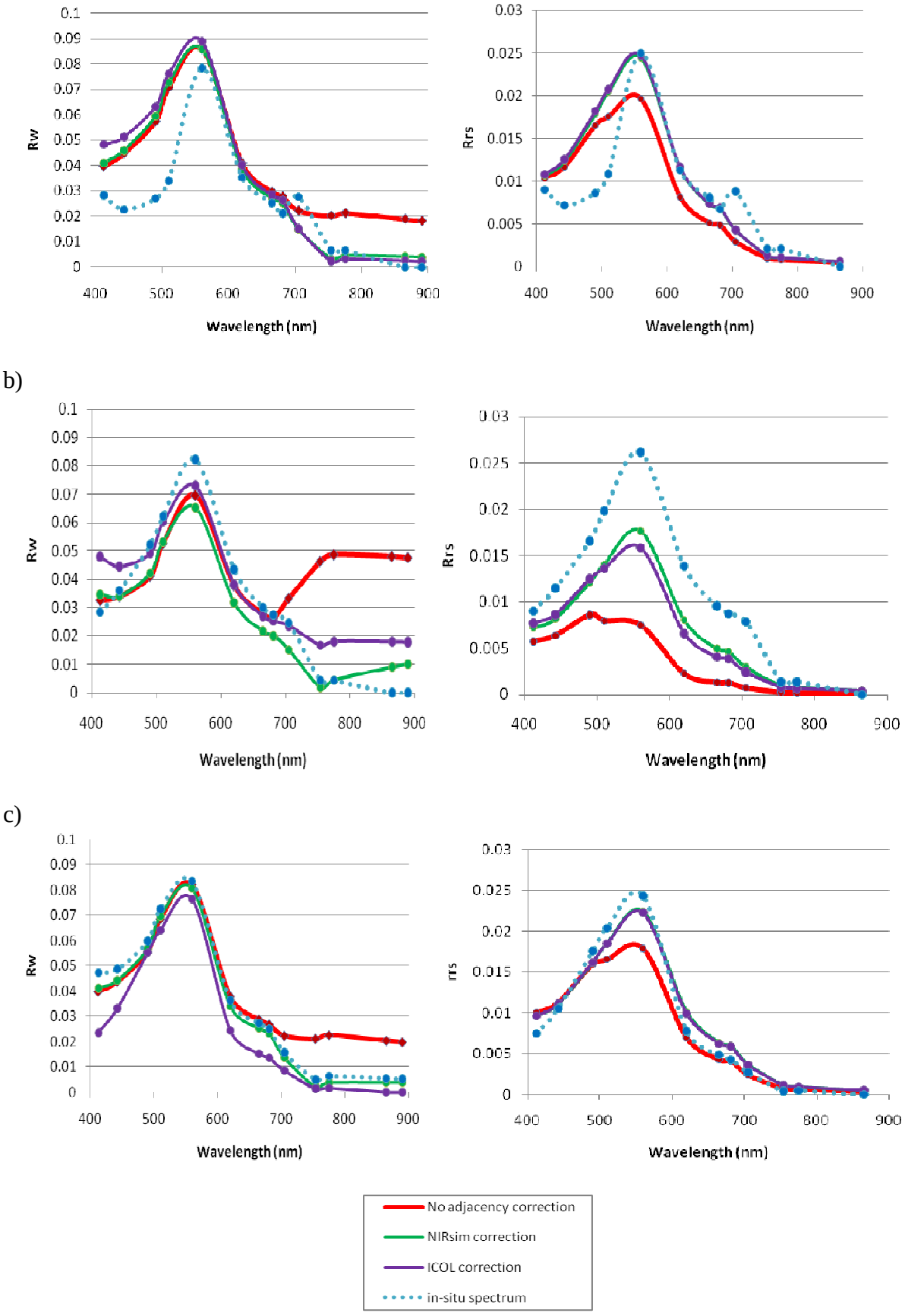

Figure 7: Comparison at Rw/Rrs level. a), b) and c) represent different locations in the lake.

CONCLUSIONS

The new SIMEC correction using the NIR similarity spectrum is shown here to be promising for the correction of MERIS data. The results presented for Lake Trasimeno give quite similar performance to the ICOL adjacency correction implemented in BEAM. To further evaluate performance more MERIS images with coincident in-situ datasets are needed for validation. In addition, as soon as the ICOL version 2.5 will be available as a public BEAM plugin new comparison excercises will be made. As a new version of Modtran (version 5) is now available with the possibility to include AOT instead of visibility a more precise intercomparison can be made.

The main future improvements will be focused on the tuning of the environment functions by regionalisation of aerosol IOPs and by incorporation of information on the aerosol vertical scale height. We will also focus on the further operationalisation of the algorithm by incorporation of SIMEC in a complete processing chain and linking it with automatic modules to derive AOT from land targets.

REFERENCES

De Haan, J.F., Kokke, J.M.M., 1996, Remote sensing algorithm development Toolkit: 1. Operationalization of atmospheric correction methods for tidal and inland waters. BCRS Report, 91 pp.

Doerffer, R., Schiller, H., 2008, MERIS regional, coastal and lake case 2 water project — Atmospheric Correction ATBD. GKSS Research Center, Geesthacht, Germany. Version 1.0, 18 May 2008.

Guanter, L., Ruiz-Verdú, A., Odermatt, D., Giardino, C., Simis, S. Estellés, V. Heege, T., Domínguez-Gómez, J.A., Moreno, J., 2010, Atmospheric correction of ENVISAT/MERIS data over inland waters: Validation for European lakes, Remote Sens. Environ., 114 (3), 467-480

Minomura, M., Kuze, H. AND Takeuch, N., 2001, Adjacency effect in the atmospheric correction of satellite remote sensing data: evaluation of the influence of aerosol extinction profiles, Optical Review, 8(2), 133-141.

Richter R., Schläpfer, D., Müller, A., 2006, An automatic atmospheric correction algorithm for visible/NIR imagery. Int. J Remote Sensing, 27(10), 2077-2085.

Ruiz-Verdu, R., S. Koponen, T. Heege, R. Doerffer, C. Brockmann, K. Kallio, T. Pyhälahti, R. Pena, A. Polvorinos, J. Heblinski, P. Ylöstalo, L. Conde, D. Odermatt, V. Estelles, J. Pulliainen, 2008, Development of MERIS lake water algorithms: Validation results from Europe. In: Proc. 2nd MERIS/AATSR workshop. Frascati, Italy.

Santer, R, Schmechtig, C., 2000, Adjacency effects on water surfaces: primary scattering approximation and sensitivity study, Applied Optics 39 (3), 361–375.

Santer, R., Zagolski, F., 2009. Improved Contrast between Ocean and Land (ICOL) algorithm theoretical basis document. Tech. rep., ULCO, Wimereux, France

Ruddick, K., De Cauwer, V., Van Mol, B., 2005, Use of the near infrared similarity reflectance spectrum for the quality control of remote sensing data. In: SPIE International Symposium on "Optics and Photonics: Remote sensing of the coastal oceanic environment", 31 July – 1 August 2005, San Diego, USA

Ruddick, K., De Cauwer, V., Park, Y., 2006, Seaborne measurements of near infrared water-leaving reflectance: The similarity spectrum for turbid waters, Limnol. Oceanogr., 51(2), 1167-1179.

Sterckx, S., Knaeps, E., Ruddick, K., 2010, Detection and Correction of Adjacency Effects in Hyperspectral Airborne Data of Coastal and Inland Waters: the Use of the Near Infrared Similarity Spectrum, Int. J. Remote Sens., accepted

Vermote E.F., Tanré D., Deuzé J.L., Herman M., Morcrette J.J., 1994, Second Simulation of the Satellite Signal in the Solar Spectrum (6S), 6S User Guide Version 6.0, (NASA-GSFC, Greenbelt, Maryland).